ELSEVIER

Polymer 41 (2000) 2613–2625

polymer

A novel epitaxy of isotactic polypropylene (α phase) on PTFE and organic substrates

S. Yan[a], F. Katzenberg[a], J. Petermann[a], D. Yang[b], Y. Shen[c], C. Straupé[c], J.C. Wittmann[c], B. Lotz[c,*]

[a]*Institute of Materials Science, Department of Chemical Engineering, University of Dortmund, D-44221 Dortmund, Germany*
[b]*Polymer Physics Laboratory, Changchun Institute of Applied Chemistry, Chinese Academy of Sciences, Changchun 130022, People's Republic of China*
[c]*Institut Charles Sadron (CNRS-ULP), 6, rue Boussingault, 67083 Strasbourg, France*

Received 17 February 1999; received in revised form 12 April 1999; accepted 16 April 1999

Abstract

Isotactic polypropylene in its α modification (αiPP) crystallises epitaxially on polytetrafluoroethylene (PTFE) and several hemiacids or salts of substituted benzoic acids via a novel contact plane, namely (110): so far, the only known contact plane involved in αiPP homo- and hetero-epitaxies was (010). In spite of its complicated architecture (alternation of antichiral helices with different azimuthal settings), the $(110)_{\alpha iPP}$ contact plane displays well defined, if not prominent, rows of methyl side chains parallel to the crystallographic ⟨112⟩ direction (at 57° to the *c*-axis) and ≈ 5.5 Å apart. The matching contact planes of the substrates display linear gratings made of rows of e.g. chlorine atoms or PTFE chains with similar ≈ 5.5 Å inter-row or interchain distances. Various morphologies are observed in iPP thin films crystallised at different cooling rates in the presence of PTFE; they can be analysed in terms of a succession and interplay of successive epitaxies: initial αiPP/PTFE heteroepitaxy, followed by αiPP/αiPP and γiPP/αiPP homoepitaxies.

Keywords: Isotactic polypropylene; Polytetrafluoroethylene; Epitaxies

1. Introduction

Epitaxial crystallisation is a widespread phenomenon in isotactic polypropylene (iPP) and is much investigated both for its scientific aspects and economic implications. Epitaxial crystallisation is documented for all three polymorphs of iPP: α, β and γ modifications, and is manifested either when iPP interacts with itself (homoepitaxy) or with "foreign" substrates (heteroepitaxy).

The best known, spontaneous *homoepitaxy* affects only the α form of iPP and results in a most spectacular and characteristic lamellar branching specific to this polymer and crystal modification [1,2]. This homoepitaxy has been analysed at a crystallographic and sub-molecular level [3,4]. It rests on an epitaxy between two (010) contact planes made of *isochiral* helices. The underlying rotation twin generates two chain orientations at 100° to each other. A similar structural relationship exists between bilayers *within the unit-cell* of the γ phase of iPP (γiPP), leading to a structure with two populations of chains with non-parallel axes [5,6]. These two chain orientations are embedded in a single lamella, and do not therefore show up morphologically in the form of lamellar branching. Finally, an epitaxy of the γ phase on the α phase has been recognised early on [7], and rests on the same pattern of crystallographic interactions.

Heteroepitaxy of iPP on various crystalline substrates and nucleating agents is used as a means to enhance the nucleation rate of the α phase [8] or to generate the more elusive β phase [9,10]. Interestingly, so far *only* the $(010)_{\alpha iPP}$ (or the equivalent $(001)_{\gamma iPP}$) contact planes involved in the *homo*-epitaxies of the α and γ phases have been found to be also involved in the *hetero*epitaxies of these phases [11]. This plane is the contact plane when a substrate periodicity of ~5 Å matches its ⟨101⟩ interrow distance, as for example in the iPP/PE or iPP/aliphatic polyamides epitaxies [12–14]. Finally, the β phase is induced by additives which display periodicities near 6.5 Å. Contrary to the previous cases, the epitaxy rests mainly on a matching with the helix axis repeat distance (≈6.5 Å) of the three-fold helices of iPP [10].

In the present article, we describe and analyse a novel type of epitaxy of iPP, which applies *exclusively* for the α phase (and *not* the γ phase). Contrary to all known epitaxies

* Corresponding author.
E-mail address: lotz@ics.u-strasbg.fr (B. Lotz)

0032-3861/00/$ - see front matter
PII: S0032-3861(99)00310-9

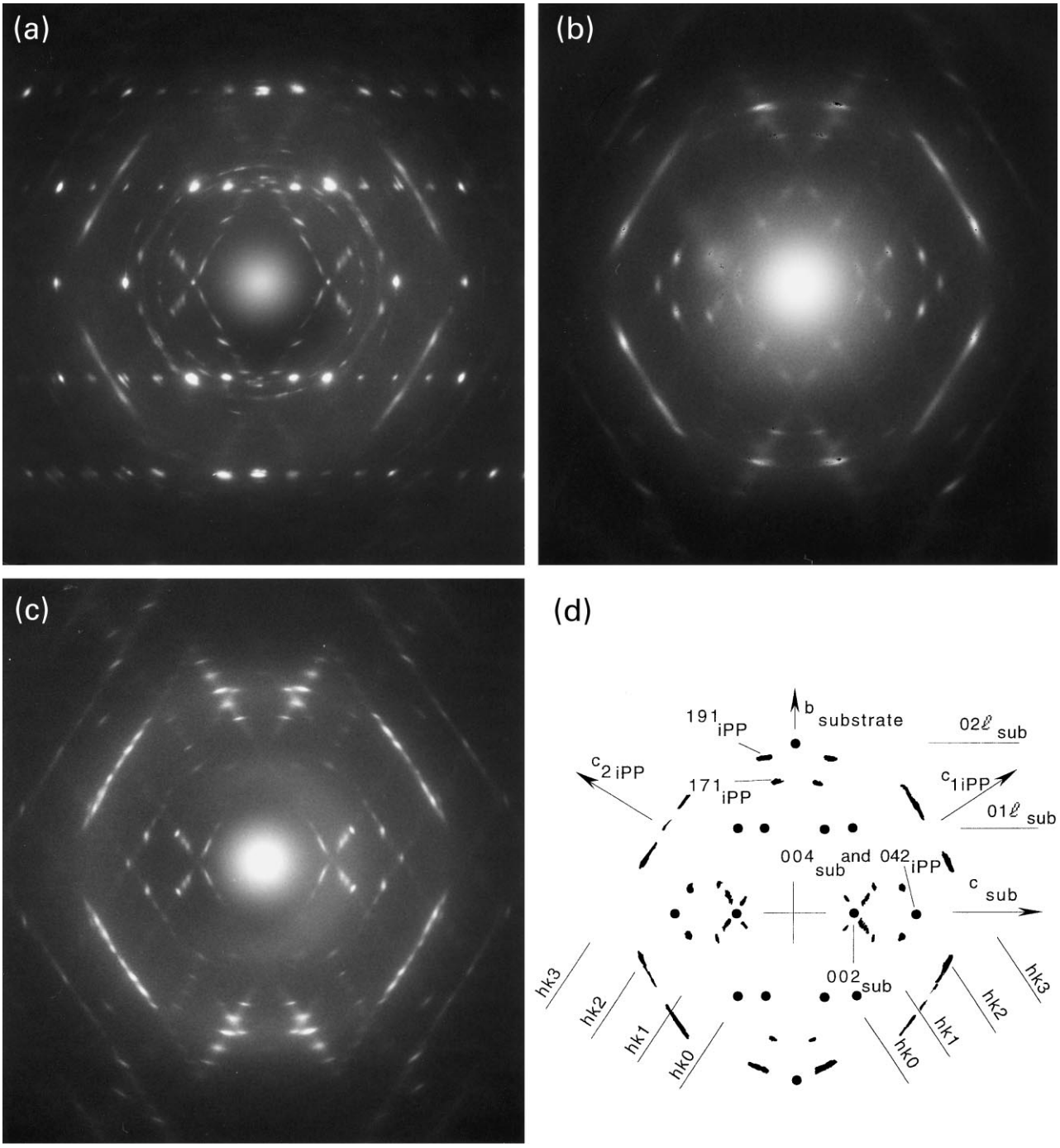

Fig. 1. (a) Selected area electron diffraction pattern (SADP) of a thin film of iPP supported by a crystal of HKClBzAc. Sharp spots and arced reflections are due to the crystal substrate and polymer, respectively. Substrate *b* and *c* axes are vertical and horizontal, respectively. Note the two chain orientations of the iPP (cf. part d). (b) SADP similar to that of part (a) after removal of the substrate by dissolution. The substrate was *p*-fluorobenzoic salt. (c) SADP as in part (b), but the iPP thin film was produced by vapour deposition of iPP heated under vacuum (thus producing low MW material) and the film has been annealed prior to dissolution of the substrate. Note the sharper iPP reflections, as well as the presence of additional, weak and broad reflections on the first layer lines (see text). (d) Schematic representation of the iPP and substrate diffraction patterns displayed in parts (a) to (c) with identification of the most important reflections.

of αiPP, the epitaxial relationship involves the $(110)_\alpha$ plane. The epitaxies are observed for a variety of substrates, both low MW ones (hemiacids or salts of substituted benzoic acid) and a polymer, namely poly(tetrafluoroethylene) (PTFE). The present investigation provides a structural explanation for the reported nucleation activity of PTFE towards iPP [15–17]. It also describes a range of complicated morphologies which are due to an interplay and succession of αiPP/PTFE heteroepitaxy and αiPP/αiPP and γiPP/αiPP homoepitaxies.

2. Experimental

Samples. Two samples of isotactic polypropylene have been used in the parallel investigations performed in the different laboratories: a sample provided by Elf-Atochem, already used in a study on enhanced nucleation [9] with MW = 315,000 and polydispersity ≈5.5, and a sample of trade name Novolene produced by BASF AG Ludwigshafen, Germany with very similar characteristics. Actually, the molecular characteristics are not of major importance in the present study, since crystallographic interactions at the unit-cell level are investigated.

Low MW organic substrates are of commercial origin, and are used without further purification. The hemiacid was produced by addition of stoechiometric amounts of the corresponding bases in methanolic solutions.

Sample preparation. Thin films of iPP are usually cast on cover glass slides from 0.5% *p*-xylene, toluene or chlorocyclopentane solutions. In some experiments, the iPP material is deposited on the substrate by vaporisation under vacuum [18]. The low MW samples thus produced yield a significantly larger proportion of γ phase [19]. Single crystals of the substrate salts, grown in a different experiment from saturated solutions (e.g. in propanol) are deposited on the polymer [20]. PTFE layers have been produced by the by now classical method of friction–deposition, in which a PTFE rod is rubbed on a glass substrate heated at some 300°C, leaving a thin (≈10–20 nm) layer of highly oriented chains with virtually single crystal orientation and organisation [21].

For crude (but often sufficient) thermal treatments, the polymer film is melted and recrystallised by sliding on a Kofler bench. In a more controlled set of experiments, notably on iPP/PTFE bilayers, thermal treatments are performed in a DSC equipment. The sample, already mounted on microscope grids, is encapsulated in a DSC pan, and the workstation of the DSC is used to monitor the thermal treatments.

The thin films are shadowed (when desired), covered with a carbon film, floated on water and mounted on copper grids. When required, calibration of the diffraction patterns is made by vaporisation of a thin layer of TlCl, although the PTFE diffraction pattern provides a convenient internal calibration via its characteristic 00 15 reflection at spacing 1.3 $Å^{-1}$ (cf. Figs. 4, 5 and 7).

Experimental techniques. Electron microscopic observations are made with Philips CM12 or CM300 instruments operated at 120 or 200 kV, respectively. Bright field images of the lamellar structure in unshadowed films are obtained through defocus of the objective lens [22].

The extensive crystal structure modelisations and analyses of diffraction patterns are performed with the relevant packages of the Cerius 2 program for molecular modelisation (Biosym-Molecular Simulations, Waltham, USA and Cambridge, UK) run on a Silicon Graphics Indigo II workstation.

3. Results and analyses

Since some morphologies are quite involved, this section presents first the results obtained with organic salts, and the structural analysis of the epitaxy is described in detail: indeed it is mostly on these substrates that a clear-cut heteroepitaxy is observed, "unspoiled" by the αiPP/αiPP homoepitaxy. This "basic" model once established is used to analyse more complex morphologies created as a result of the iPP/PTFE epitaxy, when further growth takes place in the melt and therefore involves additional iPP/iPP homoepitaxies.

3.1. Epitaxy of isotactic polypropylene on p-chloro- and p-fluoro-benzoic hemiacids

3.1.1. Crystal phase and contact plane of iPP

Fig. 1(a) shows an electron diffraction pattern obtained from a bilayer made of a thin film of iPP crystallised on top of a single crystal of the potassium hemiacid of *p*-chlorobenzoic acid (formally: potassium di-*p*-chlorobenzoate, hereafter HKClBzAc). The pattern is composed of a set of sharp spots from the salt crystal, and of small arcs from the polymer film. The spotty diffraction pattern is easily accounted for (cf. Fig. 1(d)): it corresponds to the *a* zone axis of the hemiacid, and therefore indicates that the hemiacid *bc* plane is the exposed plane, with which iPP interacts. The set of arced reflections undoubtedly indicates oriented (epitaxial) crystallization of iPP: the existence of two chain orientations, 66 or 114° apart, is best attested by the relative orientations of the more densely populated third "layer" lines. A better insight in the polymer film structure is obtained after dissolution of the substrate. Two patterns, shown in Fig. 1(b) and (c), are obtained with films produced on the chloro- and fluoro-substituted benzoic hemiacid, and with different crystallisation conditions and polymer (plain polymer and vaporised one). These patterns are unlike any previous patterns of epitaxially crystallised iPP reported so far (e.g. on benzoic acid) [12,20], and therefore indicate an original mode of epitaxial growth, based on an original contact plane. The nature of this contact plane is determined on the basis of the following observations:

- the "equators"[1] of both orientations are nearly "empty". This emptiness rules out "simple" contact planes such as (100) or (010) since prominent *hk*0 reflections would be observed.
- crucial information, best evidenced in the "simpler" pattern of Fig. 1(b), can be found on the first and second layer lines. This first layer is highly asymmetric: on one side of the meridian, a set of reflections with spacings 2.55, 2.32 and 2.1 $Å^{-1}$ can be indexed as $\bar{1}71$, $\bar{1}91$ and $\bar{1}111$ of αiPP. On the other side of the meridian, a single

[1] Equator and layer lines refer to the *hk*0 and *hkl* layer lines in case of *fiber* orientation. In the present context, it is a convenient, albeit loose terminology, since we are dealing with *single crystal* orientations.

reflection is visible, which can be indexed as 041. These diffracting planes are either exactly or nearly normal to the (110) plane: the latter is therefore the contact plane.
- in addition, the two second layer lines "intersect" at a common reflection (indicated in Fig. 1(d)) which is indexed as $0\bar{4}2$ (spacing 2.73 Å^{-1}) (indexing of the pattern in Fig. 1(d)). This set of planes is therefore common to the two αiPP populations.

Fig. 1(c), although apparently more complicated, provides essentially the same structural and orientation information. The crystallinity of iPP is higher, since the sample is made of lower molecular weight material, and it has been annealed. This shows up in particular on the third layer line in the form of sharp additional reflections. Concentring on the first layer line, we note that additional reflections are positioned between the $\bar{1}71$, $\bar{1}91$ and $\bar{1}111$ reflections mentioned above. Interestingly, these additional reflections are distinctly more diffuse than their neighbours. These reflections must be indexed as $\bar{1}61$, $\bar{1}81$ and $\bar{1}101$, again of αiPP. They are indeed expected when the packing of the *ac* layers in αiPP conforms to the $P2_1/c$ space group, i.e. when αiPP is in the more ordered so-called α'' crystal structure (see later). This phase is produced on careful annealing of the α phase. However, beyond this difference in unit-cell symmetry, the epitaxy follows exactly the pattern described above, as suggested by the presence and prominence of the crucial, superposed $0\bar{4}2$ reflections.

To sum up, the diffraction evidence gathered on iPP epitaxially crystallised on the (001) plane of the hemiacids of substituted benzoic acid indicates that the α phase of iPP is formed, and that its contact plane is (110); two iPP orientations are generated, which share a common set of $(0\bar{4}2)$ planes. As a result, the chain axes are 114° apart, and at 57° to the substrate *b*-axis orientation, as assessed by composite substrate/polymer diffraction patterns.

3.1.2. Topography of the contact faces and epitaxial interactions

3.1.2.1. Structure of the substituted benzoic acid salts and epitaxy of isotactic poly(1-butene). The crystal structure of the potassium hemiacid of *p*-chlorobenzoic acid (HKClBzAc) is known [23]. Its unit-cell parameters are: $a = 3.3$ nm, $b = 0.3846$ nm, $c = 1.121$ nm, $\alpha = \gamma = 90°$, $\beta = 89.91°$, with space group C2/c. This substrate has been used in an investigation of the epitaxy of isotactic poly(1-butene) (iPBu) in its form I′ [24]. In both earlier and present studies, the contact face of interest is the *bc* plane. As shown in Fig. 2(a), this plane is characterised by very prominent rows of chlorine atoms parallel to the *b*-axis direction, with an interrow distance equal to *c*/2, i.e. 5.6 Å. Note a second, but less marked, periodicity of 3.84 Å along the *b*-axis direction, which corresponds to the distance of stacked benzene rings.

As an introduction to the analysis of the iPP epitaxy, it is worth recalling that epitaxy of the form I′ of iPBu on HKClBzAc displays two symmetrically, tilted chain orientations, which indicate that the *helical path* of the chains is aligned parallel to the rows of chlorine atoms in the substrate contact plane [24]. The *geometrical* justification for the epitaxy rests on a dimensional matching of the interturn distance of the helix with the substrate periodicity. However, the helical path is tilted relative to the helix axis by a so-called "pitch angle", and the tilts are *symmetrical* relative to the helix axis for antichiral helices. As a consequence, epitaxy results in opposite tilts when antichiral helices are deposited on a linear grating of the substrate (Fig. 2(b)). The angle made by the two helices orientations is equal to twice the pitch angle, and therefore provides a direct measure of the helical path orientation. This relatively simple situation is exactly that observed in iPBu epitaxy, since the structure of its form I′ is based on (110) layers of *isochiral* helices, successive (110) layers being antichiral: the observed tilt of the structure therefore helps "read" in direct space the chirality of the helices in the first iPBu layer, in contact with the substrate surface [24].

3.1.2.2. Structure of αiPP and of the (110) contact plane. The analysis of the composite diffraction patterns shown in Fig. 1 indicates that the (110) contact plane of the α phase is involved in the epitaxy. It is useful at this stage to examine the main features of this (110) contact plane, and for this purpose analyse the relevant features of the αiPP crystal structure which underline the dimensional and structural polymer/substrate match involved in the epitaxial relationship.

αiPP has a monoclinic unit cell with parameters $a = 0.65$ nm, $b = 2.078$ nm, $c = 0.65$ nm, $\alpha = \gamma = 90°$, $\beta = 99.6°$, and space group either $P2_1/a$ or $C2c$ [25,26]. The αiPP crystal structure is build up of layers parallel to the *ac* plane made of *isochiral* helices which further have *the same azimuthal orientation* (in *c*-axis projection) in any one (040) or *ac* plane. However, through the operation of glide planes parallel to *ac*, successive planes along the *b*-axis are *antichiral* and the azimuthal settings of the antichiral helices are *opposite*, with one of their methyl groups pointing alternatively in the $+b$ and $-b$ directions (Fig. 3(a)). The existence of two different space group symmetries is linked with the *c*-axis "sense" of the helices in the unit-cell: if each chain location corresponds to statistical occupancy of up- and down-pointing (anticline) helices, the space group is $C2c$. This is indeed the situation which will be considered in the present analysis. However, a more ordered structure, made of anticline bilayers of isocline helices is produced on annealing and has symmetry $P2_1/a$ [27]. The two structures can be differentiated by the presence or absence of *hkl* reflections for which $h + k + l$ is even. This is indeed the major difference between the crystal phases formed under conditions which lead to Fig. 1(a) or (b) and Fig. 1(c). However, since the two structures

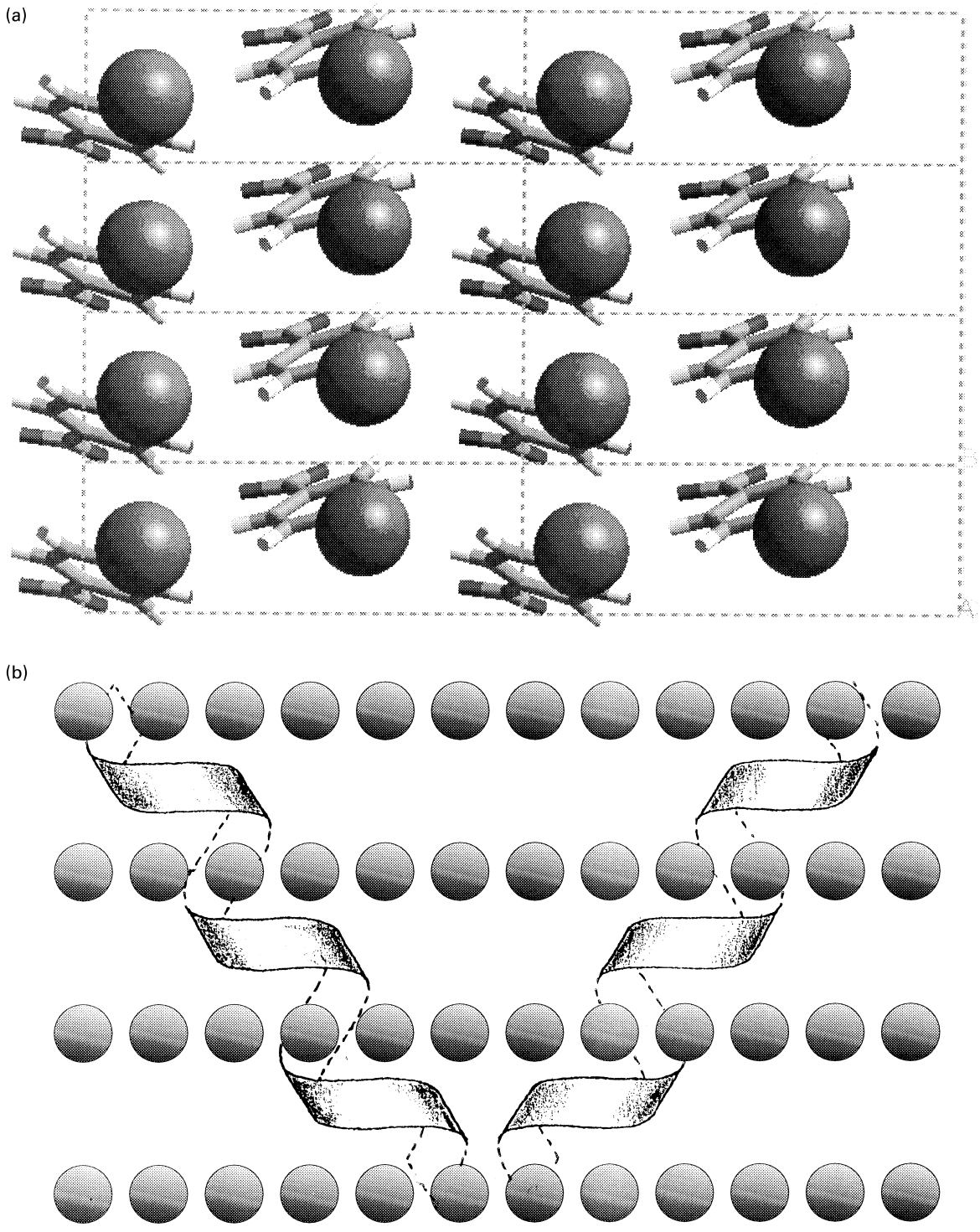

Fig. 2. (a) Computer modelisation of the (100) contact face of HKClBzAc. *b*-axis vertical, *c*-axis horizontal, in correct relative orientation to the diffraction pattern in Fig. 1(a); eight unit cells are shown. Note the prominent rows of chlorine atoms in the face, which create the (vertical) linear grating involved in the epitaxy (the diameter of chlorine atoms is 70% of the actual one). (b) Schematic drawing illustrating the tilt of right-handed and left-handed helices when the helical path interacts with a linear grating (shown here horizontal). The latter is shown in front of the helices, i.e. the viewpoint of the substrate is adopted. The helices are tilted in clock- and anticlockwise directions by the so-called pitch angle.

with different symmetries display identical epitaxies, the issue of up- or down-pointing helices is irrelevant in the analysis of the epitaxy. Indeed, this analysis is merely concerned with the methyl groups positions, which are nearly identical in up- and down-pointing helices, since anticline isochiral helices are nearly isosteric.

In all epitaxies of αiPP analysed so far, the contact plane was the *ac plane* in which only one methyl group of the

helix projects in the contact plane, as assessed by AFM [4,9,28]. This leads to a very regular, lozenge shaped array of methyl groups, which is indeed also involved in the homoepitaxy of αiPP [1–4], and is at the root of its characteristic lamellar branching [1,3].

In sharp contrast with the above situation, the (110) plane is a rather elusive plane in αiPP morphology. It is suspected to be an important growth plane, but has never been clearly identified. In the whole iPP literature, only one report shows a lamella of the α phase (grown in a 50/50 mixture of iPP and paraffin at 140°C) which displays a clear "end" growth face tilted at some 17° to the lateral *ac* or (010) faces and which was therefore identified as (110) [2]. In solution crystallisation, rectangular lath shaped crystals are formed, which build up the so-called "quadrites" [1]. These lath-shaped crystals are bound laterally by (010) faces also (which are the locations of the homoepitaxial deposition) and have "flat" ends, which suggests a growth front parallel to the lower density (100) plane. However, polymer decoration [29] indicates that the folds in this growth sector are at an angle to the end (100) faces, which in turn suggests that the macroscopic (100) growth front is actually serrated and made of much smaller (110) and ($\bar{1}$10) growth microfacets.

Whether considered in its role as a growth face or as a contact face in epitaxy, the αiPP (110) plane appears to be reasonably dense, but structurally much less regular than the (010) or *ac* plane. Since it intersects the alternating, antichiral *ac* layers packed along *b* at an angle, it is also made of an alternation of antichiral helices which, in addition, have opposite azimuthal settings (as seen in *c*-axis projection) (Fig. 3(a)). In spite of this structural complexity, the (110) face of iPP presents a distinct topological regularity.

By analogy with the earlier investigations on iPBu epitaxy [24], the existence of two populations of polymer chains tilted at an angle to each other suggests that features oblique to the helix axis are involved in the epitaxy. These however cannot be the helical path, as in iPBu, since different helices (and helical hands) are involved in the (110) contact plane. A molecular modelisation reveals nevertheless a (near) alignment of methyl side chains in that face (Fig. 3(b) and (c)): rows of methyl groups are aligned parallel to the intersection of the (0$\bar{1}$2) crystallographic plane and the (110) plane, and are 5.5 Å apart in the latter plane. Clearly, two symmetrically and structurally related planes can be considered. These correspond to the "front" and "back" sides of any one (110) plane (or ($\bar{1}$10) plane). As seen in chain axis projection in Fig. 3(a), in the "front" face, the rows of methyl groups are created by the two methyl groups located in the "base" of (for example) a right handed helix, and only one methyl group of a left handed helix, whereas the hands of the helices are opposite for the back face. The tilts of the rows in the front and back faces are symmetrically related to the *c*-axis orientation and are at 57° to that *c*-axis (Fig. 3(b) and (c)).

3.1.2.3. Epitaxial relationship The angular relationship and interrow distances just determined suggest the physical process underlying the observed epitaxy: parallel orientation of the rows of methyl groups within the (110) plane of αiPP and of a matching *linear grating* which exists in the substrate contact plane. This grating is provided by the rows of chlorine atoms parallel to the *c*-axis of the substrates and with periodicity *c*/2, i.e. 5.6 Å.

The epitaxial relationship can be formally described as:

$$(110)_{iPP}//(100)_{substrate}$$
$$\langle 112\rangle_{iPP}//\langle 010\rangle_{substrate}$$

with a one dimensional lattice match which is virtually perfect, given the periodicities involved: 5.46 $Å_{iPP}$ and 5.6 $Å_{substrate}$.

It should be further noted that the substrate periodicity normal to the one-dimensional linear grating is 3.85 Å, which is close to the 4.05 Å periodicity parallel to ⟨114⟩ of iPP, also nearly normal (but not quite: ≈96°) to the rows of methyl groups involved in the epitaxy. While this additional matching may contribute to the epitaxial relationship, it is not the determining factor, since it would lead to a slightly different, but measurable angular relationship with the substrate.

The structure of the epitaxially crystallised films can be analysed at a very detailed level, paralleling in this respect a similar analysis made for the homoepitaxial crystallisation of αiPP onto itself [3,9]. In particular, it is possible to determine which role is played by the right-handed and left-handed helices interacting with the substrate, i.e. to determine if they interact with only one, or with two methyl groups with that substrate. In this reasoning, we follow also closely the analysis made for the iPBu epitaxy, recalled earlier (Fig. 2(b)), and which leads to the recognition of the hand of helices in contact with the substrate [24]. With the help also of Fig. 3(b) and (c), we note that the orientation of the rows of methyl groups in the (110) face relative to the *c*-axis direction is close to that of the helical path of helices lying "flat on" in the contact plane, i.e. of helices which interact with two methyl groups with the substrate. Adopting the viewpoint of the substrate and looking *at* the iPP deposit, it is clear that the helix axis is rotated *anticlockwise* relative to the row of (chlorine) atoms which exist in the substrate if these helices are right handed (Fig. 3(b)), and it is rotated *clockwise* for left-handed helices (Fig. 3(c)). This simple geometrical argument helps therefore determine the chirality and the "role" (azimuthal setting, defined by the flat-on orientation or not) of *every* helix in the contact face-and by extension, the azimuthal setting and hand of *every* helix in the bulk of the polymer film since, in the α phase structure, all helices of the same hand have identical azimuthal settings.

To conclude this section, we stress that the epitaxial relationship determined here involves a (110) contact plane of αiPP that had not been observed so far. A major characteristic of the contact face is the coexistence of antichiral

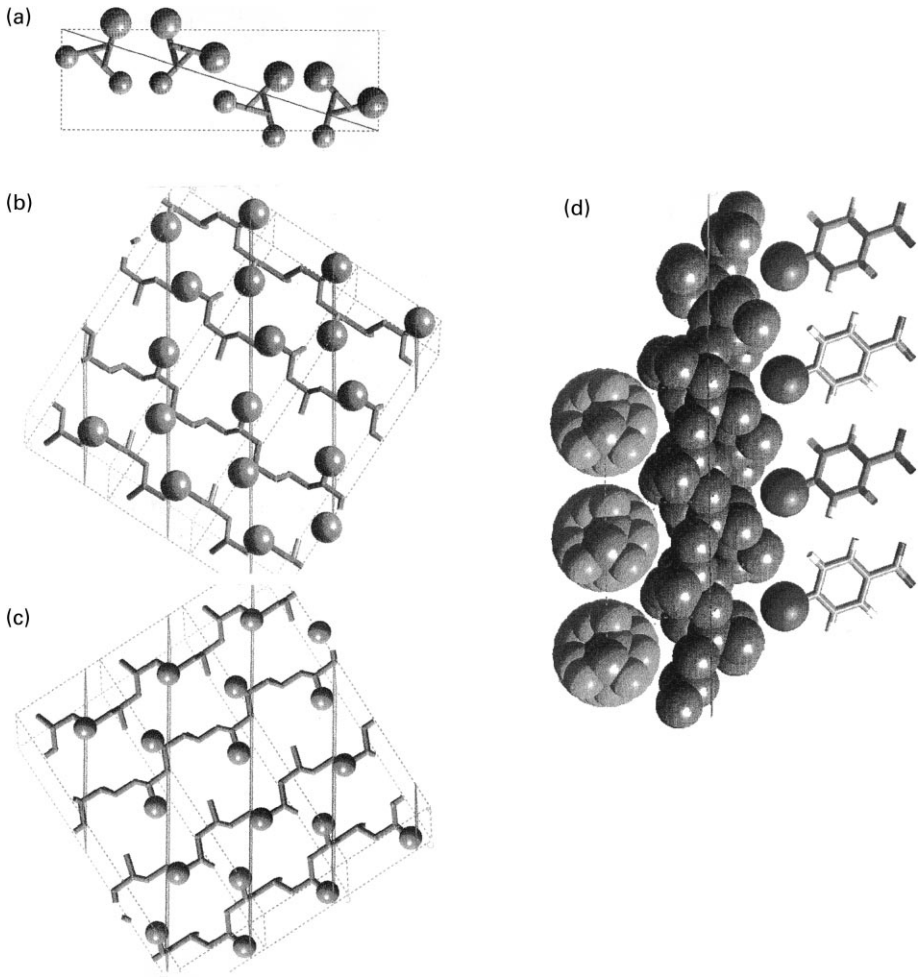

Fig. 3. (a) Crystal structure of the α phase of iPP, as seen down the chain axis. Successive helices along the *b*-axis are antichiral. The methyl groups (carbon atoms only are shown) located in the "front" and "back" (or top and bottom) sides of the ($\bar{1}$10) plane (chosen here for convenience) are represented with different diameters. (b) (c) Plane-on views of the rows of methyl groups in the "top" (b) and bottom (c) faces of the ($\bar{1}$10) plane of αiPP in (a). The hand of helices displaying two methyl groups can be "read" directly from the model: right-handed in (b), left-handed in (c). The family of (021) planes (spacing: ≈ 5.5 Å) is represented, and is aligned vertically, as for the diffraction patterns in Fig. 1. Note the symmetric 57° off vertical tilt of the iPP chain axes in (b) and (c). (d) Schematic illustration of the epitaxial interactions between the iPP (110) layer shown in (a–c) and HKClBzAc and PTFE. The iPP layer in (b) and (c) is seen from the bottom, along $\langle 112 \rangle_{iPP}$, the HKClBzAc along *b*, and PTFE along the chain axis direction.

helices with different azimuthal settings, and up–down statistical substitution of isochiral helices. In spite of these rather adverse features, the positions of the methyl side groups are sufficiently constrained in the αiPP crystal structure as to create a linear grating with a ≈ 5.5 Å periodicity. The linear grating of methyl groups is involved in the epitaxial process with substrates with a matching grating (for example rows of chlorine atoms) of similar periodicity (Fig. 3(d)). The substrates investigated so far are low MW organic materials or salts. As examined now, similar epitaxies are observed when the second component is a polymer, namely PTFE.

3.2. iPP/PTFE epitaxy

It is known since nearly 30 years that PTFE fibres or films can nucleate the crystallisation of iPP in its α modification [15]. This nucleation ability is quite effective, since it takes place up to temperatures (e.g. 152°C) at which "spontaneous" (heterogeneous) nucleation of iPP is limited, thus leading (for PTFE fibres immersed in undercooled iPP) to cylindrical transcrystalline αiPP growth over several hundred μm [16].

However, these extensive studies of iPP/'PTFE systems have not led to a molecular understanding of the interactions between the two polymers. Recent scanning electron micrographs of the PTFE fibres revealed fissures, which were thought to increase the number of "active nucleation sites", but were also suspected "not to be solely responsible for the formation of transcrystallinity" [16]. In a more recent report of the same group, thermal-stress induced orientation and relaxation of polymer chains was invoked, in association with small-scale grooves on the PTFE fibres [17].

Our approach to the analysis of iPP/PTFE interactions

rests again on the formation and examination by electron microscopy and diffraction of thin bilayers of the two polymers. In the present case, we are helped by the availability of the friction-transfer deposition of PTFE on solid supports [21], which produces thin, highly oriented and even single crystalline layers with exposed (10.0) planes, and with a thickness (a few nm) perfectly suited for the present study by transmission electron microscopy and electron diffraction [9]. In this section, our results on the iPP/PTFE system are presented and it is shown that the resulting morphology depends on the crystallisation temperature (or cooling rate). The fast quenched systems can be analysed essentially as for the above systems and are described first. The morphology and diffraction patterns of films crystallised at higher temperatures analysed next are more complex, since the homoepitaxy characteristic of αiPP growth (which generates lamellar branches) comes into play.

3.2.1. iPP/PTFE: fast crystallisation rates

When crystallisation of the molten iPP takes place in the lower part of the crystallisation range (i.e. between ≈ 100 and 120°C), the resulting lamellar morphology is reminiscent of, but significantly different from, the standard "cross hatched" morphology characteristic of pure iPP [1,4]. Indeed, the film is made of two sets of crystalline lamellae several μm long standing *edge on* on the PTFE film, but with an angle different from the characteristic 80 or 100° indicative of the homoepitaxy (Fig. 4(a)).

Electron diffraction patterns reveal the presence of the underlying PTFE film, which is hidden in the bright field micrograph of Fig. 4(a). The pattern (Fig. 4(b)) can be analysed in a straightforward manner: it is indeed a superposition of the diffraction pattern of the PTFE film itself and of the patterns analysed above for the iPP epitaxy on HKClBzAc, as revealed by the trademark 171 and 191 reflections near the "fibre" axis of PTFE, at the level of its 7th and 8th layer line streaks.

The underlying epitaxial relationship is similar to that described for the salt substrates. In the present case, the linear grating is created by the PTFE molecules, which are 5.5 Å apart in the exposed (100) plane rather than by rows of chlorine atoms. The epitaxial relationship is thus described by:

$$(110)_{iPP}//(100)_{PTFE}$$
$$\langle 112\rangle_{iPP}//\langle 001\rangle_{PTFE}$$

and the one dimensional lattice match between iPP and PTFE is again virtually perfect, since the spacings are within 0.1 Å of each other.

3.2.2. iPP/PTFE epitaxy: moderate and slow cooling rates

The nucleation ability of PTFE towards iPP is reduced in the higher crystallisation temperatures range [16]. In the present set of experiments, this effect is illustrated by using different cooling rates. To help the analysis developed

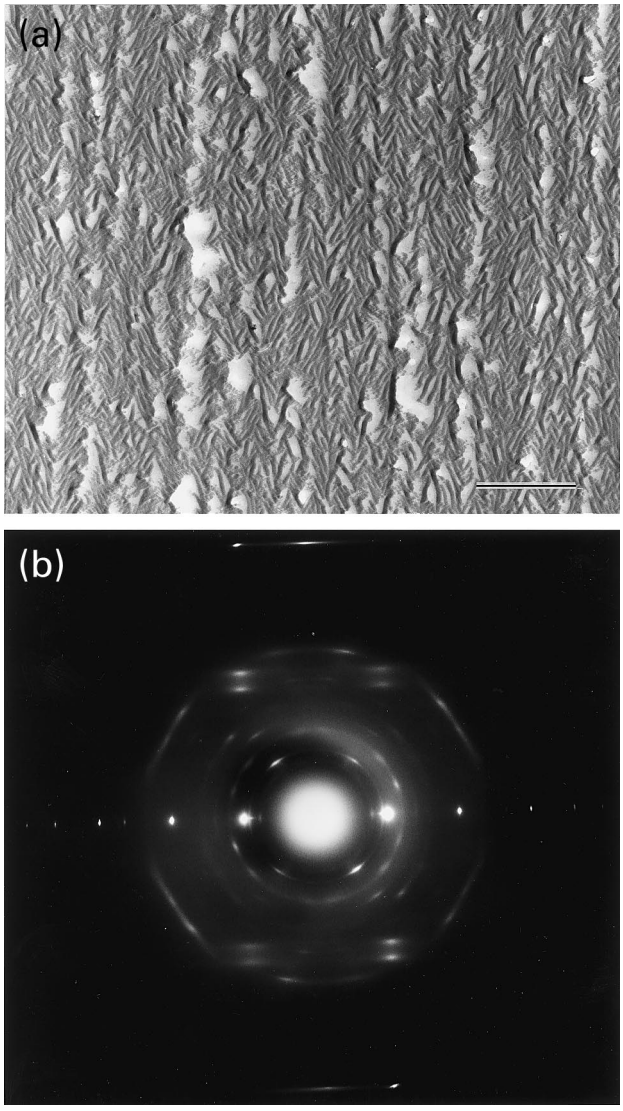

Fig. 4. (a) Transmission electron micrograph of a thin film of iPP epitaxially grown on a substrate layer of rubbed PTFE (chain axis orientation vertical). Pt/Carbon shadowing at $tg^{-1} = 1/3$. Scale bar: 1 μm. (b) Electron diffraction pattern of a film as in part (a). PTFE chain axis vertical; chain axes orientations of the two populations of iPP and analysis of the pattern as in Fig. 1(d) (Note however the more prominent presence of 040_{iPP} reflections).

next, it is useful at this stage to anticipate its conclusions. The experimental evidence indicates that in addition to the iPP/PTFE heteroepitaxy analysed so far, the conventional αiPP/αiPP homoepitaxy comes into play. It takes place on the (010) edges of the PTFE-nucleated iPP lamellae and generates a second population of nearly *flat-on* lamellae, which however keeps an orientation memory of the initial iPP/PTFE nucleation step. This process is here illustrated for two different cooling rates. The first (hereafter "moderate cooling") is not well controlled: it amounts to taking an electron microscope grid with the iPP/PTFE bilayer mounted on a carbon film out of the DSC oven at 185°C, and letting it cool in ambient air. The second (hereafter "slow cooling") involves a cooling rate of 10°C/min of

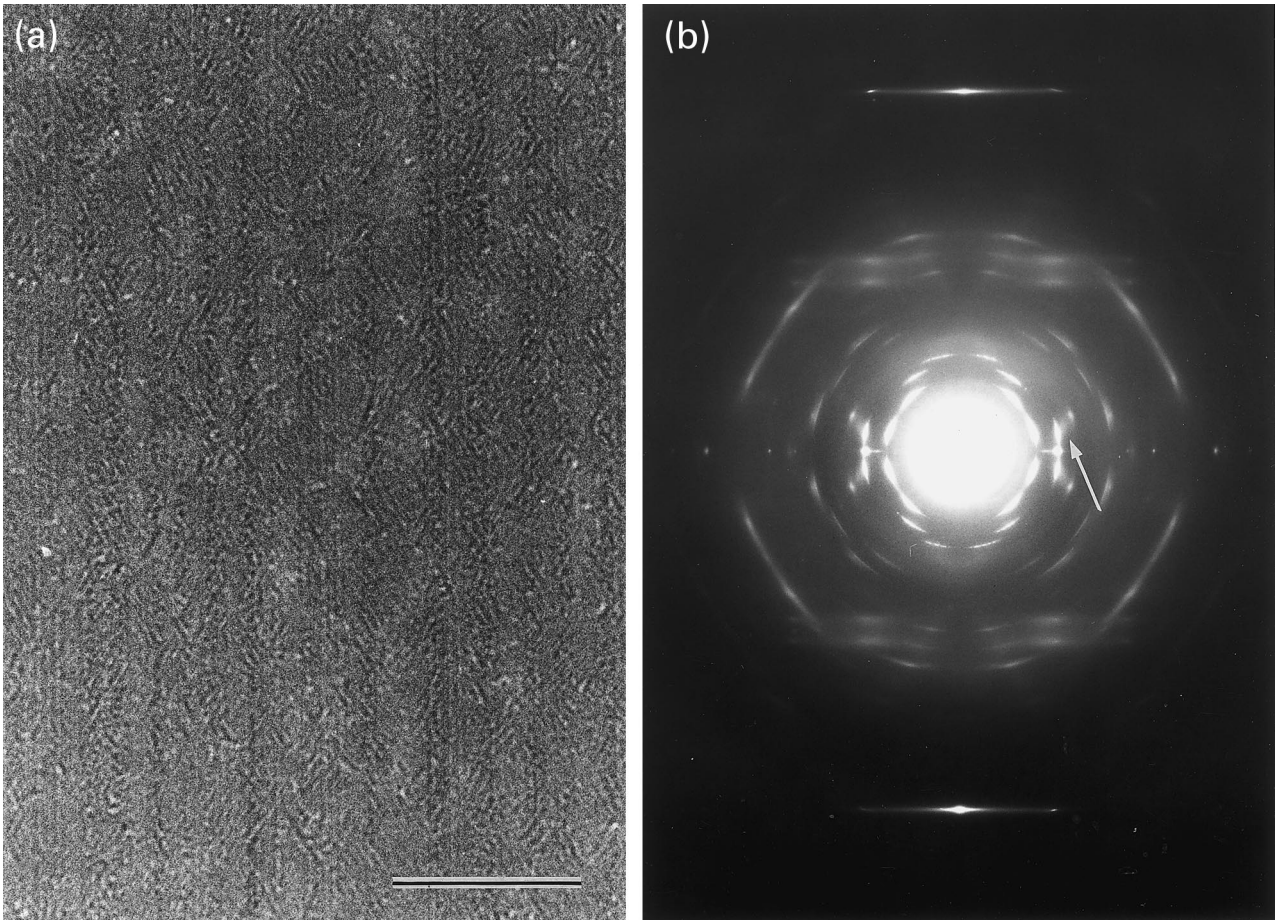

Fig. 5. (a) Transmission electron micrograph (defocus mode) of a thin film of iPP deposited on a PTFE oriented film, and crystallised by moderate cooling. The defocus mode highlights the sole population of edge-on lamellae Note however the existence of rather featureless domains which indicate flat-on lamellar growth as well. Scale bar: 0.5 μm. (b) SAED pattern of a film as in part (a). Note the presence of two very prominent sets of additional *hk*0 reflections, indicating flat-on lamellar growth, and their orientation parallel to the "layer-lines" of the initial iPP growth, indicating αiPP/αiPP homoepitaxial growth. One of the characteristic 117_{γ} reflections, slightly outside the $130_{\alpha iPP}$ reflection, is arrowed. Note that contrary to the bright-field pictures, the diffraction pattern emphasises the flat-on lamellae, which yield higher intensity *hk*0 reflections.

a similar grid stored in a DSC pan, using the thermal regulation of the DSC workstation.

On moderate cooling, the iPP film is again made of two populations of edge-on lamellae, as revealed by the defocused bright field picture shown in Fig. 5(a). However, significant portions of the film appear rather featureless. They correspond to regions of the (thin) film in which lamellae have grown *flat-on*. The presence of this population of lamellae is best revealed by electron diffraction (Fig. 5(b)). This pattern appears at first sight rather complicated, but its analysis is straightforward. It displays the reflections of the two polymers (PTFE and iPP), the latter making up four populations of lamellae, symmetrically oriented relative to the PTFE chain axis. The by now familiar PTFE substrate has its chain axis vertical; the two populations of iPP lamellae generated by the iPP/PTFE epitaxy are revealed by the faint, characteristic reflections on the first and second layer lines, as analysed above; finally, two populations of lamellae are at the origin of the new features in the pattern: very prominent *hk*0 reflections of αiPP (110, 130, 040, …). These extra reflections are in a very characteristic orientation relative to the two populations of the epitaxially oriented lamellae of αiPP: the 1*k*0 reflections (110, 130) are located on the *first layer line* (*hk*1) of the two epitaxially oriented iPPs (cf. Fig. 1(d)), and the *a*-axis of the new populations of lamellae is parallel to the *c*-axis of the edge-on lamellae. This relative orientation of the two crystalline lattices is a trademark of the homoepitaxy taking place on the lateral (010) faces of αiPP, which results in an interchange of *a* and *c* axes orientations in the parent and daughter lattices across the contact plane, while the *b*-axis orientation is preserved [1,3,4]. The new populations of lamellae will be described as "second generation" iPP lamellae.

In the first generation of iPP lamellae (i.e. epitaxially crystallised on PTFE), the *ac* plane is oriented at some 75° to the film surface. As a result of the iPP/iPP homoepitaxy, the "second generation" of iPP lamellae is build up of chains that are at only 10° to the substrate surface normal, with the *a*-axis parallel to the film surface, and with the *b*-axis also tilted to the film surface (Fig. 6). Through growth,

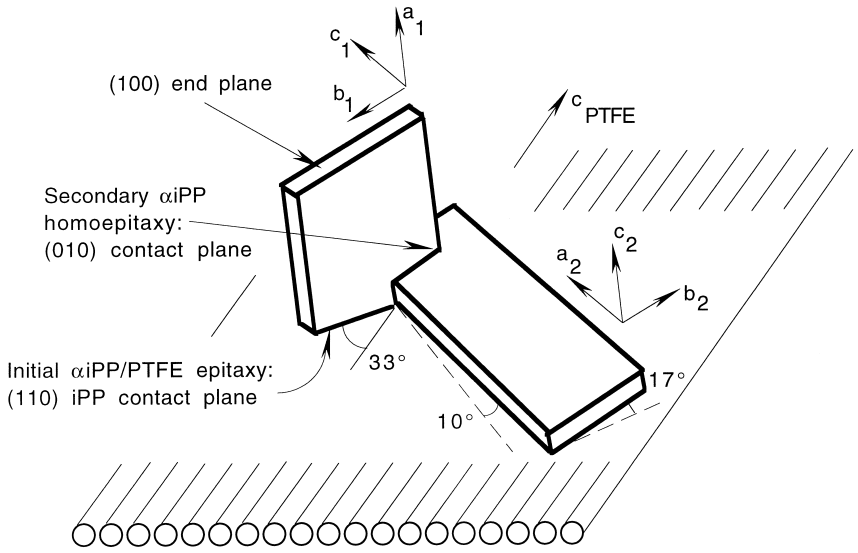

Fig. 6. Schematic drawing of the epitaxial relationship between PTFE and iPP, and the orientation of second generation iPP lamellae through αiPP/αiPP homoepitaxy. PTFE chains are shown as cylinders. The initial (110) epitaxy of iPP sets the unit-cell orientation in the vertical lamella: c_1 parallel to the substrate plane, b_1 at 17° to that plane, a_1 at 80 or 100° (i.e. the β(angle of the monoclinic unit-cell) to it. Through the αiPP/αiPP epitaxy, the a_2, b_2, c_2 axes are collinear with the c_1, b_1 and a_1 axes. The plane of the second generation lamellae is therefore slightly out of the substrate plane (angles of 10° and 17°, assuming that the chains are normal to the αiPP lamellar surface). In thin film growth, the lamellae reorient parallel to the substrate surface, and yield the prominent patterns shown in Figs. 5(a) and 7(a). This schematic drawing represents only one of the two symmetrically related families of parent and daughter lamellae. The drawing is inaccurate on at least two grounds: (a) the (100) end planes are represented, only to help perceive the lamellar geometry. While observed in solution crystallisation, they are not characteristic of melt growth; (b) the back *ac* growth faces of lamellae 1 and 2 should be nearly in the same plane. Indeed, assuming that nucleation of lamella 2 took place on the back growth face of lamella 1, the growth rates of the two faces are thereafter equal. This observation also helps locate the actual (010) homoepitaxy contact plane *strictly* at the geometric centre of the daughter lamella 2.

mainly along the a^*-axis, which is by far the fastest growth direction in αiPP, these lamellae tend to lie flat-on (i.e. parallel to the substrate surface which acts as a physical support), *but keep the memory of the initial b-axis orientation* (in projection onto the film surface, i.e. as seen in electron diffraction): this relative orientation of unit-cells and of parent and daughter populations of lamellae is an *unambiguous marker* of the αiPP/αiPP homoepitaxial origin of the daughter (second generation) populations.

From the analysis of Fig. 5(a) and (b), we therefore conclude that, at moderate cooling rates, PTFE is an efficient nucleating agent for iPP. Through this initial iPP/PTFE epitaxy, two populations of αiPP lamellae are generated, which are symmetrically oriented relative to the PTFE chain axis direction. However, the density of nucleation is reduced: the uncrystallised material is prone to crystallise through the (presumably energetically favoured) αiPP/αiPP homoepitaxy. The presence, and relative proportion of the latter population of flat-on lamellae actually provides an indication—qualitative but reliable—about the local crystallisation conditions, as also illustrated for the slow cooling rates examined now.

For slow-cooling rates, i.e. when the thin iPP/PTFE composite film mounted on EM grids is cooled at 10°C/min in a DSC pan, the defocused bright field images (Fig. 7(a)) indicate the presence of relatively large domains (in the μm^2 or several μm^2 range) with a *single* orientation of the edge-on iPP lamellae. Electron diffraction patterns on any *one* domain (Fig. 7(b)) show a faint indication of edge-on lamellae and a substantial proportion of flat-on lamellae, as evidenced by the prominence of the *hk*0 reflections, and the trademark 57° orientation to the PTFE *c*-axis. This orientation confirms that the flat-on lamellae are in homoepitaxial relationship with the edge-on ones, as schematised in Fig. 6 and are therefore of second generation.

In addition to this major fraction of two lamellar orientations at + and −57° to the PTFE *c*-axis, a third population of domains exists with edge-on lamellae, this time oriented nearly (but not quite) *at right angles to the PTFE chain axis* (Fig. 7(a), left hand side). Such domains are however relatively rare, and their existence cannot be analysed on the basis of any satisfactory lattice matching. While this population has not been analysed with the same detail as the (110) epitaxy, it would appear that we are dealing with some type of "graphoepitaxy" induced by the surface topology (perhaps some form of crevices inferred by Wang and Hwang [16]). It is not possible at this stage to develop further this analysis, beyond mentioning the existence of this third population of domains and a possible nucleation mechanism which appears to have a very limited impact in the overall nucleation process of PTFE towards αiPP.

The "single crystalline" orientation of lamellae in domains several μm^2 indicates that the density of nucleation is reduced at these lower cooling rates (or higher T_cs), in agreement with the more global observations of Wang and

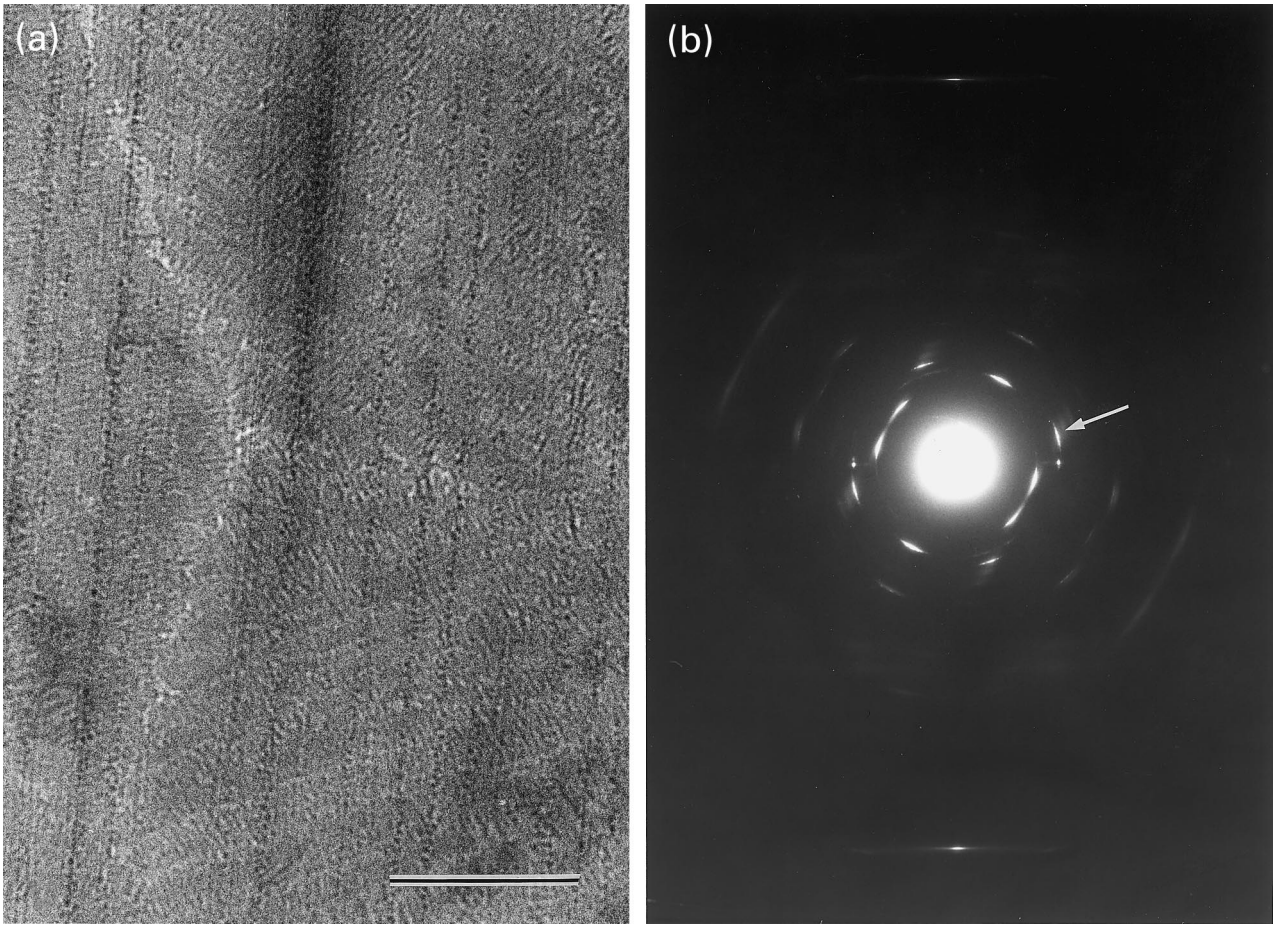

Fig. 7. (a) Transmission electron micrograph of a thin film of iPP deposited on a PTFE oriented film, and crystallised by cooling at 10°C/min in a DSC pan. The field of view is occupied by only three "monodomains", indicating reduced nucleation frequency. One of the monodomains (right hand side) has an infrequent orientation of lamellae, roughly normal to the PTFE chain axis direction (a second set of lamellae, nearly parallel to the PTFE chain axis is probable, but not easily visible in this imaging mode: the overall lamellar pattern would therefore correspond to a quadrite structure seen along the common *b*-axis). Scale bar: 0.5 μm. (b) SAED pattern of the top left portion of the film in part (a), in proper relative orientation. Note the presence of only one set of additional *hk*0 reflections, which demonstrates a single nucleation event, and the characteristic tilt of the pattern relative to the PTFE chain axis, indicative of αiPP/PTFE epitaxy. One 117_{γ} reflection arrowed.

Liu [17]. However, the mere size and shape of these domains raises an interesting issue about the nucleation and growth of iPP in the thin films. Indeed, since the orientation is homogeneous over the whole domain, the nucleation must be a single event and the growth process spreads the orientation information associated with the epitaxial nucleation. In the thin films investigated in this study, and keeping in mind that growth is much faster along the a^*-axis, this spread can hardly take place through the growth of the first (edge-on) generation of lamellae, since the a^*-axis is nearly normal to the film surface: this spread must mainly take place through the growth of the daughter (second generation) lamellae, which have their *a* axes oriented in the film plane. For bulk crystallisation however, such as PTFE fibres embedded in molten iPP [17], it is the first generation lamellae (with their fast growth a^*-axis nearly normal to the PTFE surface) which contribute mainly to defining the transcrystalline growth of iPP on the PTFE fibres.

Before concluding this section, it is also worth emphasising that the diffraction patterns display in most cases a set of reflections at 4.4 $Å^{-1}$, which is a trademark indicator of the γ phase of iPP (indexed as 117 in the cell of Brückner and Meille [5]). One of these reflections is arrowed in Figs. 5(b) and 7(b). Their presence confirms that after the initial epitaxial nucleation step, growth of iPP is essentially identical to the bulk crystallisation: in particular, the lower MW material crystallises in this γ phase, probably during the later stages of the crystallisation process. An exhaustive analysis of these populations of γ phase material is not necessary in the present context, beyond noting that the location of these 117 γ phase reflections confirms that this phase is in the "standard" γ/α epitaxial relationship, which has been analysed in quite detail previously [19].

3.3. The (110) epitaxy in the context of other αiPP epitaxies

It is of interest to examine the newly demonstrated

epitaxy in the broader context of epitaxial crystallisation of the various crystal phases of isotactic polypropylene. At present, three iPP contact planes have been documented, which are characterised by periodicities close to 5 Å, 6.5 Å and the newly observed 5.6 Å, and match similar substrates periodicities:

- for substrate periodicities of 5 Å, as observed in benzoic acid and its salts, but also polyethylene, aliphatic polyamides,… iPP crystallises in the α phase, with a (010) contact plane [12,13]. These substrates *can also nucleate directly the γ phase*, since the $(080)_\gamma$ plane is structurally similar to the $(010)_\alpha$ one [4,9]. The epitaxial relationships highlight the rather simple organisation of methyl groups of iPP in a lozenge-type array in the *ac* contact plane, which is made of isochiral helices. Although the helix path is barely "felt" by the substrate, the chirality of the helices in the contact plane can be determined through the tilt of the chain axis relative to the substrate grating—at least for the α phase (the γ phase helix axes are symmetrically oriented relative to that grating, which does not allow determination of the hand of helices in the contact plane) [4,9].
- for substrate periodicities of 6.5 Å, as exist in γ-quinacridone and several more recent β phase nucleating agents, iPP crystallises in the β phase. The epitaxial relationship rests on a one dimensional match with the chain axis repeat distance of iPP, in sharp contrast with the above epitaxy [11]. The topography of the (110) contact face of βiPP is more complex, in view of the different azimuthal settings of helices in that plane, which reflects the frustrated nature of the crystal structure [30], but the contact plane is also made of isochiral helices. The hand of the helices cannot be determined, since the *helix axes* (rather than the *helical path*) align with the substrate grating.
- for periodicities of 5.6 Å (the substrates investigated in this study, including PTFE), the contact face is $(110)_{\alpha iPP}$. The contact face is made of an alternation of antichiral helices. Since the helix axes are oblique to the substrate linear grating, the helical hand of each helix can be determined. Interestingly however, there is no structural equivalent of this $(110)_{\alpha iPP}$ plane for the γ phase, which also means that *the nucleating agents considered in the present investigation are specific for the α phase of iPP*. For the γ phase indeed, only $(00l)_\gamma$ layers can be involved in epitaxial relationships, since *only in these planes* are the helix axes *parallel* to the contact plane—a constant feature of all epitaxies involving polymers. By contrast, the non-parallel orientation of helices axes in successive (004) bilayers of the γ phase implies that *all* non-$(00l)_\gamma$ crystallographic planes "intersect" one chain out of two in the crystal lattice, which rules out these planes for epitaxy: some of the chains would have to stay "erect" in the contact plane and "impinge" into the contact plane of the substrate. However, as shown in the present study by the presence of its characteristic 117 diffraction spots, the γ phase can be produced on the α phase nucleated first on PTFE through the conventional γ/α epitaxy.

Finally, in the broader context of polymer/polymer epitaxies, it should be mentioned that the new periodicity of 5.6 Å is a "common denominator" of αiPP, PTFE and isotactic poly(1-butene) (in its form I or I′) and may well be involved in nucleation or crystal transformations observed in binary mixtures of these polymers. For the binary system iPP/iPBu however, parallelism of the chain axis directions suggests that the matching of identical *c*-axis repeat distances characteristic of 3-fold polyolefin helices (6.5 Å) is the major contributing factor [31].

4. Conclusion

A novel mode of epitaxial crystallisation of iPP has been observed and analysed. The novel epitaxial relationship is generated by substrates which display in their exposed faces a linear grating of periodicity 5.5–5.6 Å. Representative examples of such gratings are the rows of chlorine atoms in the (100) plane of salts or hemiacids of *para* substituted benzoic acid, or the interchain distance of PTFE helices. This linear grating is matched in the $(110)_{\alpha iPP}$ contact plane by rows of methyl groups with a comparable interrow distance. Interestingly, in spite of the fact that the contact face is made of exposed methyls attached to both right- and left-handed helices with different azimuthal settings as well as statistical up–down orientations, the structural (topological) regularity of these planes is sufficient to allow epitaxy. As in most epitaxies in which the helical path is involved in the epitaxial match, the deposition of these iPP helices is a "chiral" process, which makes it possible to deduce the hand of individual helices in the contact plane, based on the sole relative orientation of iPP helix axes and substrate "rows", materialised for example by the PTFE chains.

The present epitaxial relationship adds a third "dimensional standard" of 5.5–5.6 Å to the set of two previously known iPP hetero- or homo-epitaxies, which are based on distances of 5 Å and 6.5 Å. Whereas the 5 Å periodicity applies to both homo- and heteroepitaxies of the α and γ phases, the 6.5 Å periodicity generates only the β phase polymorph, and the newly uncovered 5.6 Å periodicity generates exclusively the α phase (but not the γ phase). In the broader context of structure and morphology studies of isotactic polypropylene, the present study illustrates the role of the (110) plane, which was suspected to be important in α phase iPP growth, but had almost never been clearly identified. Interestingly, its major structural features have been brought to light by the analysis of its role as a contact plane in epitaxy.

References

[1] Khoury FJ. Res Natl Bur Stand Sect A 1966;70A:29.
[2] Padden Jr FJ, Keith HD. J Appl Phys 1966;37:4013.
[3] Lotz B, Wittmann JC. J Polym Sci B: Polym Phys 1986;24:1541.
[4] Stocker W, Magonov SN, Cantow HJ, Wittmann JC, Lotz B. Macromolecules 1993;26:5915 Correction: 1994; 27: 6690.
[5] Bruckner S, Meille SV. Nature 1989;340:455.
[6] Meille SV, Bruckner S, Porzio W. Macromolecules 1990;23:4114.
[7] Padden Jr FJ, Keith HD. J Appl Phys 1973;44:1217.
[8] Fillon B, Wittmann JC, Lotz B, Thierry A. J Polym Sci B: Polym Phys 1993;31:1383.
[9] Lotz B, Wittmann JC, Lovinger AJ. Polymer 1996;37:4979.
[10] Leugering HJ. Makromol Chem 1967;109:204.
[11] Stocker W, Schumacher M, Graff S, Thierry A, Wittmann JC, Lotz B. Macromolecules 1998;31:807.
[12] Petermann J, Gross B. J Mater Sci 1984;19:105.
[13] Lotz B, Wittmann JC. J Polym Sci B: Polym Phys 1986;24:1559.
[14] Lotz B, Wittmann JC. J Polym Sci B: Polym Phys 1987;25:1079.
[15] Fitchum DR, Newman S. J Polym Sci A-2 1970;8:1545.
[16] Wang C, Hwang LM. J Polym Sci B: Polym Phys 1996;34:47.
[17] Wang C, Liu C-R. Polymer 1998;40:289.
[18] Ashida M, Ueda Y, Watanabe T. J Polym Sci Polym Phys Ed 1978;16:179.
[19] Lotz B, Graff S, Straupé C, Wittmann JC. Polymer 1991;32:2902.
[20] Wittmann JC, Lotz B. Prog Polym Sci 1990;15:909.
[21] Wittmann JC, Smith P. Nature 1991;352:414.
[22] Petermann J, Gleiter H. Phil Mag 1975;31:929.
[23] Mills HH, Speakman JC. J Chem Soc 1963:4355.
[24] Kopp S, Wittmann JC, Lotz B. Polymer 1994;35:916.
[25] Natta G, Corradini P. Nuovo Cim Suppl 1960;15:40.
[26] Bruckner S, Meille SV, Petraccone V, Pirozzi B. Prog Polym Sci 1991;16:361.
[27] Corradini P, Giunchi G, Petraccone V, Pirozzi B, Vidal HM. Gazz Chim Ital 1980;110:413.
[28] Stocker W, Lovinger AJ, Schumacher M, Graff S, Wittmann JC, Lotz B. ACS Symp Seri, 694, chap. 3, 1998:53.
[29] Wittmann JC, Lotz B. J Polym Sci Polym Phys Ed 1985;23:205.
[30] Dorset DL, McCourt MP, Kopp S, Schumacher M, Okihara T, Lotz B. Polymer 1998;39:6331.
[31] Boor Jr. J, Mitchell JC. J Polym Sci Lett 1962;62:S70.